JOURNAL OF MATERIALS SCIENCE 1 (1966) 142–153

Differential Thermal Analysis and X-ray Diffraction Study of Devitrification Processes

Part 2 Li_2O-Al_2O_3-B_2O_3-SiO_2 Solder Glasses

L. F. OLDFIELD, D. J. HARWOOD, B. LEWIS
The General Electric Co Ltd, Central Research Laboratories, Hirst Research Centre, Wembley, UK

Received 22 October 1965

This paper describes the use of DTA, in conjunction with fibre softening point measurements, in determining suitable solder glass compositions for the manufacture of devitrifiable seals to conventional glasses. The range of compositions examined was: 0 to 17 Li_2O; 21 to 44 Al_2O_3; 0 to 23 B_2O_3; 29 to 47 SiO_2; 0 to 12 MgO; 0 to 24 Na_2O; 0 to 22 K_2O; and 0 or 17 P_2O_5 wt%.

X-ray diffraction analysis of the devitrification products formed after heat treatment at the respective DTA main exotherm temperatures showed that, in most glasses, the major crystalline phase present had the β-eucryptite-type structure. Variations in the unit cell dimensions of this phase accompanied the changes in nominal glass compositions. In glasses containing large proportions of sodium oxide, the major devitrification product was of the nephelite type.

1. Introduction

The devitrification of lithia-alumina-silica glasses has been investigated extensively, and many of the glass-ceramics made have proved to be of technical importance. The two major crystalline phases formed, namely, tetragonal β-spodumene ($Li_2O.Al_2O_3.4SiO_2$) and hexagonal β-eucryptite ($Li_2O.Al_2O_3.2SiO_2$), have low or negative thermal expansions and relatively high melting points. The glass-ceramics therefore have good thermal shock resistance, are more refractory than the original glasses, and have much higher mechanical strength.

β-Eucryptite has a structure similar to that of high- or β-quartz and is sometimes described as the silica-O form of eucryptite. In many accounts of the devitrification of lithia-alumina-silica glasses, this crystalline phase has also been denoted as β-eucryptite/quartz solid solution and the high silica phase as β-spodumene/quartz solid solution [1]. In the following account, we have chosen to denote the crystalline phase observed in the glass-ceramics as a β-eucryptite-type phase. This takes into account the measurable differences in crystal lattice dimensions compared with those of synthetic β-eucryptite. The magnitude of these differences varies slightly from one glass composition to another.

The devitrification of glasses in the magnesia-alumina-silica system has produced glass-ceramics with medium to low thermal expansion coefficients, good electrical insulation and high mechanical strength. These properties have been attributed by McMillan [1] to the presence of α-cordierite ($2MgO.2Al_2O_3.5SiO_2$) as the principal phase.

2. Solder Glass-Ceramics

The above systems can be combined and further modified to give solder glass-ceramics covering a wide range of thermal expansions, although some of the advantages of the ternary composi-

tions (such as high mechanical strength and refractoriness) are reduced in favour of certain other desirable properties [2].

A solder glass-ceramic, sometimes known as a devitrifiable glass solder, is made from a glass which is sufficiently fluid to wet a standard sealing glass at a temperature at which the latter does not deform. The former is used in a manner similar to that employed for a standard solder glass, but, on suitable heat treatment (also at a temperature at which the standard glass does not deform), it is devitrified to a more refractory material which must be compatible in thermal expansion/contraction properties with the sealing glass. The sealing and heat treatment temperatures are not necessarily the same. In this way, many useful combinations of glass-to-glass, glass-to-metal and glass-to-ceramic seals can be made. In some cases, an expansion mis-match is desirable; for example, the strengthening of a standard glass can be achieved by casing a layer of a lower expansion solder glass-ceramic onto it. If, in addition, the solder glass-ceramic is more refractory than the standard glass, then the cased glass will deform at a higher temperature than the former [3].

In most applications, the other main requirements for the devitrified glass solder are as follows:

(a) It must not soften at a lower temperature than the glass or ceramic to which it is sealed, so that standard vacuum baking schedules for the latter can be maintained.

(b) It must not devitrify before sealing has been effected.

(c) The seals which it forms with the other materials must be at least equal in strength to conventional glass seals.

(d) The seals must be hermetic or vacuum tight.

A solder glass-ceramic is normally used as a slurry of fine grains, ~ 5 μm diameter, in an organic suspension medium and applied to the surfaces to be sealed by dipping or painting. The suspension material is volatilised before the sealing temperature is reached. Similar or related compositions can be used for pressed and sintered compacts by using a material of coarser grain size and a much smaller quantity of organic binder. As devitrification in the absence of deliberate heterogeneous nucleation usually proceeds more rapidly at the surface than in the bulk glass, a given volume of compacted glass powder can be devitrified more quickly than the same volume of bulk glass.

A non-porous body can only be made from a slurry or powder compact if sintering between grains has preceded devitrification, and it is preferable that a small percentage of glassy matrix remains after crystallisation is complete to ensure minimum porosity. Sintering normally begins in the region of the Littleton fibre softening point at a viscosity of $10^{7.6}$ poises [5].

These solder glass-ceramics can therefore be distinguished from many glass-ceramics which are preformed into bulk glass articles by conventional techniques. In these cases, it is preferable to carry out devitrification below the Littleton point so that sagging or deformation does not occur.

3. Experimental

3.1. Differential Thermal Analysis (D T A)

This method can be used for the rapid determination of the devitrification temperature and of the liquidus of the resulting phases; the former giving an exothermic peak and the latter an endothermic peak. The technique has been described previously [4]. In most cases, the useful limits for devitrification lie between ~ 20 to 30° C below the devitrification peak and ~ 30 to 50° C below the endothermic peak. The latter peak is normally the temperature limit for the solder glass-ceramic seal.

The investigation to be described in the following section illustrates how DTA was used in conjunction with softening point measurements to distinguish compositions which may be useful as glass solder ceramics, from those which have no possible use in this connexion.

3.2. Solder Glass Compositions

Five series of glasses were melted for the DTA investigation. The modifications were as follows:

Series 1 – Base glass, B11: Al_2O_3 30; SiO_2 42; Li_2O 9; B_2O_3 19 wt %. Glasses B21, 31, 41, 51: Li_2O substituted for B_2O_3 in B11 glass in 2% stages (Li_2O 11 to 17%; B_2O_3 17 to 11%).

Series 2 – Base glass, B11. Glasses B12 to B16: MgO substituted for SiO_2 in 2% stages (MgO 2 to 10%; SiO_2 40 to 32%).

Series 3 – Boric oxide was omitted, but lead oxide was partially substituted for it to maintain fluidity and to increase the thermal expansion coefficient. Base glass, A1: Al_2O_3 32; SiO_2 47; PbO 8; Li_2O 11; MgO 2 wt %. Glasses A2 to A6: MgO substituted for Li_2O in 2% stages (MgO 4 to 12%; Li_2O 9 to 1%).

Series 4 – Base glass, D1: Al_2O_3 23.4; SiO_2 34.8; MgO 7.6; B_2O_3 17.9; Li_2O 0.9; Na_2O 15.4 wt%. Glasses D2 to D8: Li_2O was increased at the expense of Na_2O to give a linear decrease in thermal expansion through the series; the remaining constituents were also increased.

Series 5 – Base glass, E1: Al_2O_3 21.7; SiO_2 32.2; MgO 7.0; B_2O_3 16.6; Li_2O 0.9; K_2O 21.6 wt%. Glasses E2 to E8: Li_2O was increased at the expense of K_2O to give a linear decrease in thermal expansion through the series; the remaining constituents were also increased.

The composition details are given in tables I and II. Further related series of glasses (B101, 103, 105; AA13, 23, 40, 41; C133, 135; BP111 to BP116) were also melted, and these are described below with reference to the X-ray analysis of the sintered products. The composition details are given in table III.

The glasses were melted and prepared for DTA and X-ray diffraction studies as described previously [4]. 3 g samples were used in each DTA run. Littleton fibre softening points were measured in the normal manner [5].

4. Results

4.1. Series 1: B11 to B51

The substitution of Li_2O for B_2O_3 decreased the temperature of the exothermic peak through the series from 707 to 548° C; the peak height increased markedly but the peak width decreased (figs. 1 and 2). The endothermic peak was present only in the glasses containing less than 17% B_2O_3; the increase in Li_2O producing a decrease from 760 to 745° C in the peak temperature. The annealing dip also decreased in temperature and became more pronounced with increasing Li_2O content.

The exothermic peak and softening point temperatures are compared in fig. 2. The fibre softening point is below the exothermic peak temperature only for the low lithia glasses B11 and 21, containing 19 and 17% B_2O_3 respectively. B51 glass containing 17% Li_2O and 11% B_2O_3 devitrified before the softening point could be measured. Compositions B31, 41 and 51 are therefore not suitable for solder glass-ceramics.

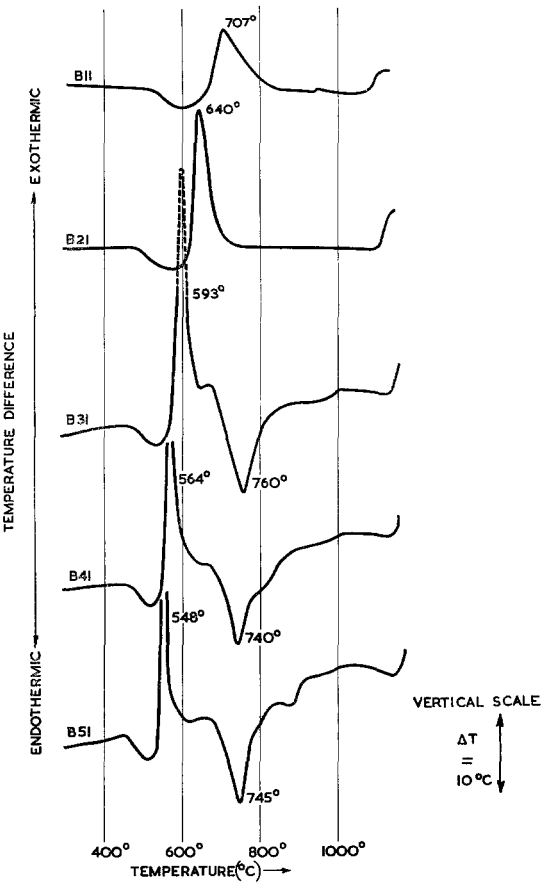

Figure 1 DTA of Li_2O-Al_2O_3-B_2O_3-SiO_2 glasses. Series 1. Substitution of Li_2O for B_2O_3.

TABLE I Li_2O-Al_2O_3-SiO_2 glasses. Series 1 modified by B_2O_3; B glasses. Series 3 modified by PbO and MgO; A glasses. Wt% compositions.

	B11	B21	B31	B41	B51	A1	A2	A3	A4	A5	A6
Al_2O_3	30	30	30	30	30	32	32	32	32	32	32
SiO_2	42	42	42	42	42	47	47	47	47	47	47
Li_2O	9	11	13	15	17	11	9	7	5	3	1
B_2O_3	19	17	15	13	11	—	—	—	—	—	—
PbO	—	—	—	—	—	8	8	8	8	8	8
MgO	—	—	—	—	—	2	4	6	8	10	12

TABLE II Wt % compositions and X-ray analyses of devitrified Li_2O-Al_2O_3-SiO_2-MgO-B_2O_3 glasses. Series 2, 4, and 5.

Series	Al_2O_3	SiO_2	MgO	Li_2O	B_2O_3	Na_2O	K_2O	Heat treatment		Principal phase	Secondary phase(s)	
								Hours	°C		Quantity	Constitution
2												
B11	30	42	—	9	19	—	—	2	700	Hexagonal β-eucryptite	—	—
B12	30	40	2	9	19	—	—	1½	690	,,	Very weak	The secondary phases have not been completely identified. Some magnesium metaborate $Mg(BO_2)_2$ is observed.
B13	30	38	4	9	19	—	—	1½	690	,,	Weak	
B14	30	36	6	9	19	—	—	1¾	680	,,	Weak to medium (10 to 15 wt%)	In both samples the secondary phase is essentially $Mg(BO_2)_2$. A very small quantity of additional crystalline material is present.
B15	30	34	8	9	19	—	—	½	660	,,	Medium (20 to 30 wt%	
B16	30	32	10	9	19	—	—	—	—	—	—	—
4												
D1	23.4	34.8	7.6	0.9	17.9	15.4	—	1	750	Nephelite type	—	—
D2	23.6	35.2	7.6	1.9	18.1	13.6	—	—	—	—	—	—
D3	23.9	35.5	7.7	2.9	18.2	11.8	—	2	750	Equal amounts of nephelite type and β-eucryptite type	—	—
D4	24.2	35.8	7.8	3.9	18.4	9.9	—	—	—	—	—	—
D5	24.4	36.2	7.8	4.9	18.6	8.1	—	—	—	—	—	—
D6	24.6	36.6	8.0	5.9	18.8	6.1	—	2	675	Equal amounts of nephelite type and β-eucryptite type.	—	—
D7	24.9	37.0	8.1	6.9	19.0	4.1	—	—	—	—	—	—
D8	25.1	37.4	8.1	8.1	19.2	2.1	—	½	675	β-Eucryptite type	Weak to medium	β-Spodumene and magnesium metaborate $Mg(BO_2)_2$.
5												
E1	21.7	32.2	7.0	0.9	16.6	—	21.6	—	—	—	—	—
E2	22.1	32.9	7.2	1.7	16.9	—	19.2	—	—	—	—	—
E3	22.5	33.5	7.3	2.7	17.2	—	16.8	8	750	$Mg(BO_2)_2$ and β-eucryptite type	Weak	Potassium magnesium silicate type.
E4	23.0	34.2	7.4	3.7	17.5	—	14.2	8	750	β-Eucryptite type	Moderate weak	$Mg(BO_2)_2$ + potassium magnesium silicate type.
E5	23.4	34.8	7.6	4.7	17.9	—	11.6	—	—	—	—	—
E6	23.9	35.5	7.7	5.7	18.2	—	8.9	2	710	β-Eucryptite type	Moderate	$Mg(BO_2)_2$
E7	24.4	36.3	7.9	6.8	18.6	—	6.0	1	670	—	—	—
E8	24.9	37.0	8.0	8.0	19.0	—	3.1	—	—	—	—	—

TABLE III Wt % compositions and X-ray analyses of further series of devitrified Li_2O-Al_2O_3-SiO_2-MgO-B_2O_3 glasses.

Series	Al_2O_3	SiO_2	MgO	Li_2O	B_2O_3	P_2O_5	Heat treatment Hours	Heat treatment °C	Principal phase	Secondary phases
B101	25	45	—	7	23		3	725	β-Eucryptite type	25% tetragonal β-spodumene + very small quantity of unidentified phase.
B103	25	41	4	7	23		3	725	,,	Small amount of β-spodumene + phase similar to magnesium metaborate $Mg(BO_2)_2$
B105	25	37	8	7	23		3	725	,,	
AA13	42	32	2	9	15		2	720	,,	Unidentified phase
AA23	44	32	—	9	15		2	720	,,	
AA40	40	32	8	5	17		4	835	Tetragonal β-spodumene (~ 50 μm crystals)	Unidentified phase of crystallite size ~ 1 μm, possibly magnesium or aluminium borate
AA41	38	32	8	5	19		4	835	,,	
BP111	27.4	38.3	—	8.2	8.6	17.4	2	750	β-Eucryptite type	Very weak unidentified phase
BP112	27.4	36.5	1.8	8.2	8.6	17.4	2	750	,,	Very weak
BP113	27.4	34.7	3.6	8.2	8.6	17.4	2	725	,,	Weak
BP114	27.4	32.8	5.5	8.2	8.6	17.4	2	725	,,	Medium (20 to 30%)
BP115	27.4	31.1	7.3	8.2	8.6	17.4	2	700	,,	Medium
BP116	27.4	29.2	9.1	8.2	8.6	17.4	2	700	,,	Medium 30%
				Na_2O						Same phase, unidentified, but different from weak phase in 111. Possibly magnesium phosphate.
C133	22.3	36.6	3.6	24	13.5		4	730	Nephelite type	Not identified
C135	22.3	33.0	7.2	24	13.5		4	730	,,	

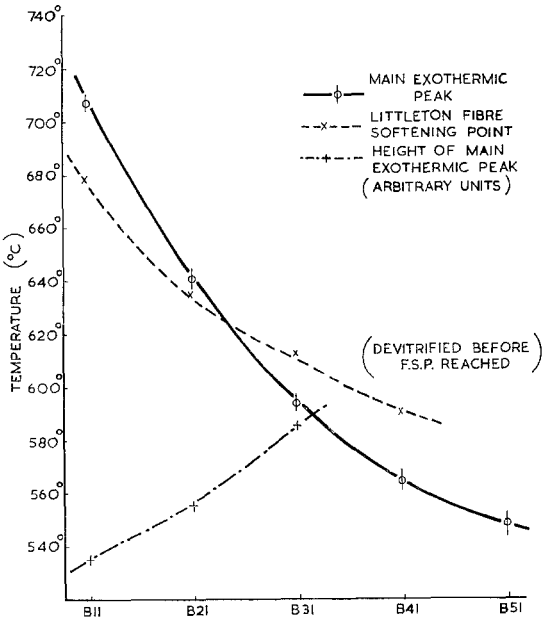

Figure 2 Li_2O-Al_2O_3-B_2O_3-SiO_2 glasses. Series 1. Substitution of Li_2O for B_2O_3. Variation of main exothermic peak, peak height and fibre softening point with composition.

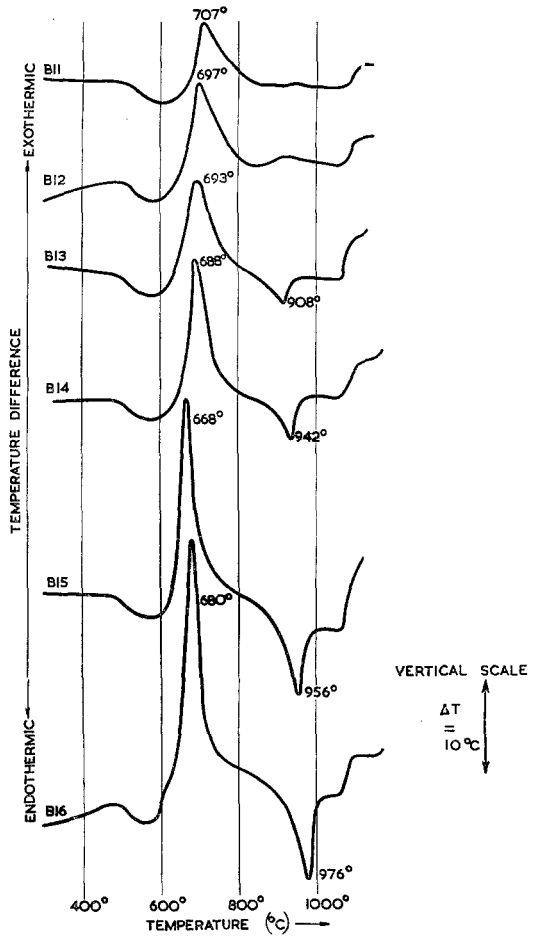

Figure 3 DTA of Li_2O-Al_2O_3-B_2O_3-SiO_2 glasses. Series 2 Substitution of MgO for SiO_2.

4.2. Series 2: B11 to B16

The substitution of MgO for SiO_2 decreased the exothermic peak temperature and increased the peak height (figs. 3 and 4). The endothermic peak became defined at 4% MgO and this increased in height and in temperature from 908 to 976° C through the remainder of the series. The fibre softening point remained well below the exothermic peak temperature for this series (fig. 4). A change in behaviour of the exotherm and the softening point occurred between 6 and 8% MgO. This is at present not fully explained, but has also been noted in similar series of glasses containing magnesia (Al_2O_3 25; Li_2O 5; B_2O_3 19; SiO_2 47 to 41; MgO 4 to 10 wt%) in which a change also occurred between 6 and 8% MgO. It may be due to the occurrence of a significant proportion of Mg $(BO_2)_2$ in the devitrification product, and this is discussed below. The expansion coefficients of the sintered products were in the range $\sim$ 1.0 to 2.0 $\times$ 10^{-6}/°C in this series.

4.3. Series 3: A1 to A6

The first substitution of 2% MgO reduced the main exothermic peak temperature by about 70° C, but further increases in MgO increased the peak temperature from 613 to 876° C (fig. 5) and decreased the peak height. A second exothermic peak appeared at 920° C for 8% MgO, and this became stronger with increasing MgO and was the dominant peak at 12% MgO, with a peak temperature of 1000° C. Rather small endotherms were shown by A3 to A5, but these were not apparent below 1100° C for A1, A2 and A6.

All these glasses devitrified before the respective fibre softening point was reached and would not therefore sinter in a satisfactory manner. It was noted that the viscosity at higher temperatures increased as MgO was substituted progressively for Li_2O. As this series was not successful, no X-ray diffraction analyses were carried out on the sintered products.

4.4. Series 4: D1 to D8

This system of glasses was devised to give

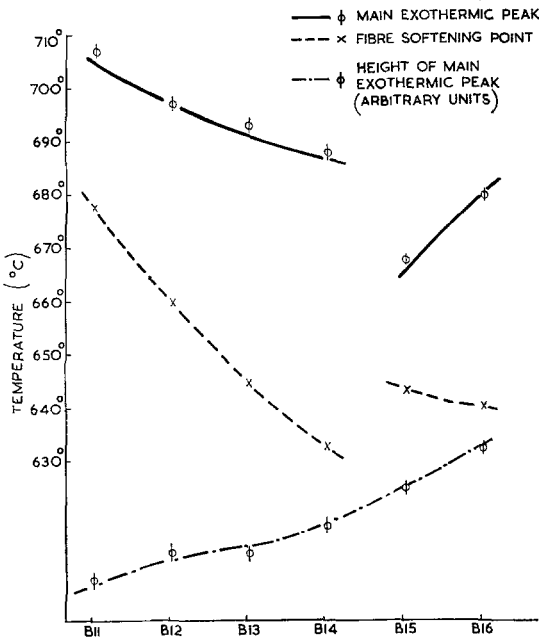

Figure 4 Li_2O-Al_2O_3-B_2O_3-SiO_2 glasses. Series 2. Substitution of MgO for SiO_2. Variation of main exothermic peak, peak height and fibre softening point with composition.

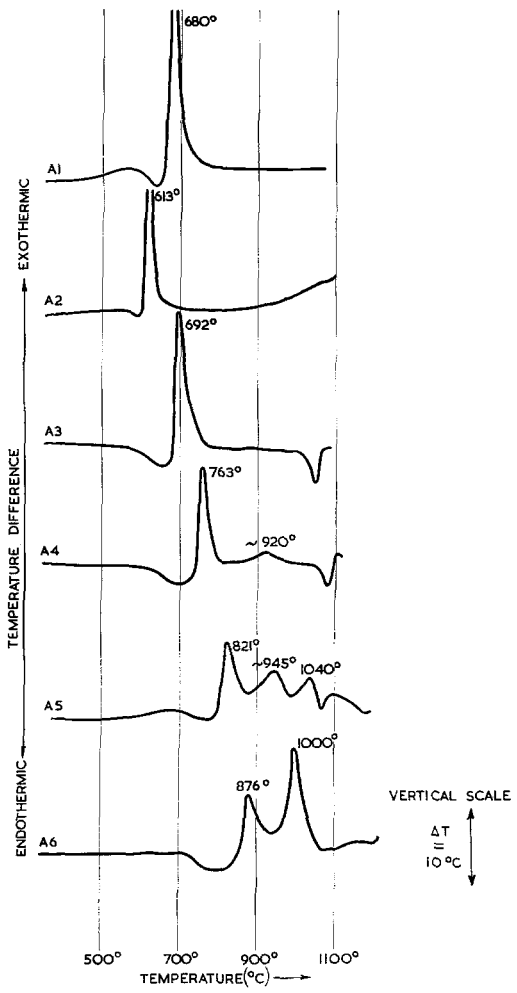

Figure 5 DTA of Li_2O-Al_2O_3-SiO_2-PbO glasses. Series 3. Substitution of MgO for Li_2O.

sintered products with thermal expansion coefficients covering the range 2 to 12 $\times$ 10^{-6}/°C. All the glasses gave relatively strong exothermic peaks which varied from 753° C through 770 to 738° C, as the Li_2O content increased from 0.9 to 3.9% and the Na_2O content decreased from 15.4 to 9.9% (fig. 6). A second peak appeared in D4 at 770° C and this also appeared in D6 at 705° C. In glasses D5 to D8, the exothermic peak changed in appearance and steadily decreased in temperature from 681 to 654° C.

The endothermic peaks were also well defined and decreased steadily from 950° C for D1 to 865° C for D5. Again a change in appearance occurred and this peak increased in temperature to 949° C for D8.

All the exothermic peaks were above the fibre softening points, denoted by F in fig. 6. Sintered products could be made successfully and these showed a linear change in expansion coefficient through the series (fig. 7).

4.5. Series 5: E1 to E8

This system was also devised to give sintered products covering a wide expansion range, but was not as successful as series 4, although the softening points were below the devitrification peaks. The DTA thermograms in fig. 8 show that the devitrification peaks in the potassium-rich glasses were poorly developed and pronounced peaks only occurred with glasses richer in Li_2O than E5, which contained 4.7% Li_2O and 11.6% K_2O. Steady trends were shown by the series E5 to E8; the exotherms increasing in height and decreasing in temperature from 747 to 664° C; the endotherms decreased in height but increased in temperature from 942 to 962° C. The exotherms are very similar to those for equivalent glasses in the D series. The sintered products of compositions E4 to E7 showed a linear change in expansion coefficient from 8 to 4 $\times$ 10^{-6}/°C.

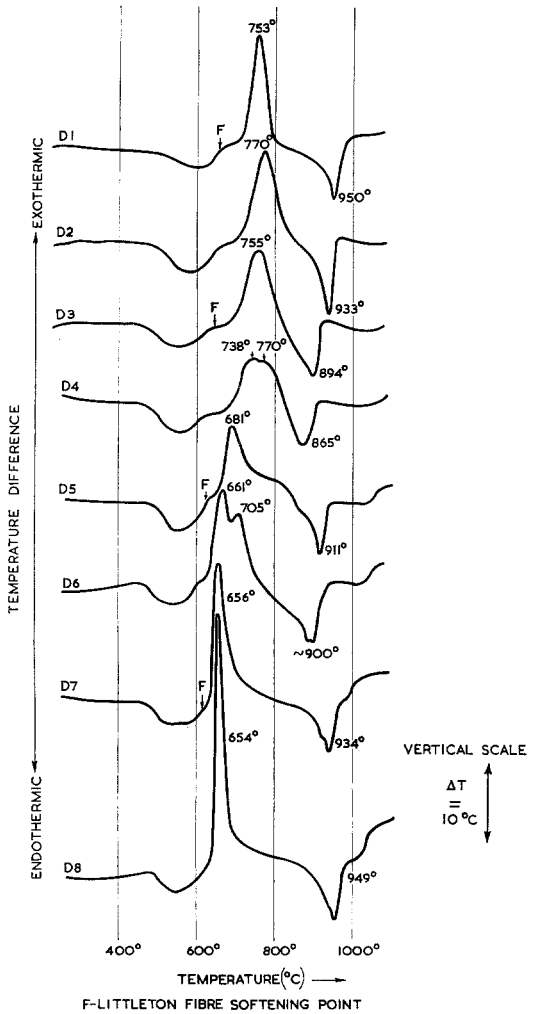

Figure 6 DTA of Na_2O-Li_2O-Al_2O_3-B_2O_3-SiO_2-MgO glasses. Series 4.

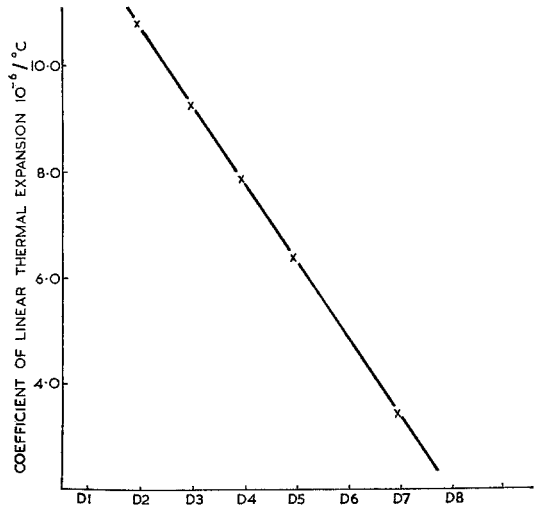

Figure 7 Na_2O-Li_2O-Al_2O_3-B_2O_3-SiO_2-MgO glasses. Series 4. Variation of linear thermal expansion coefficient of sintered and devitrified product with Na_2O and Li_2O content.

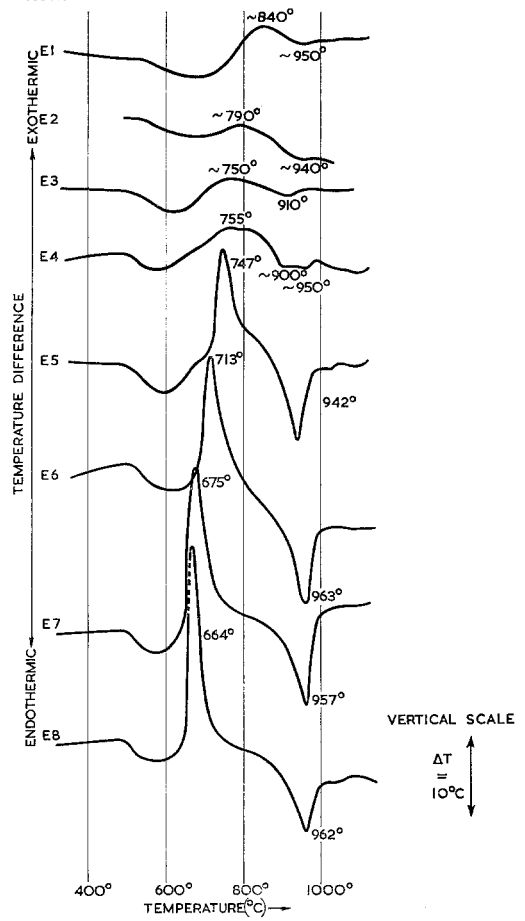

Figure 8 DTA of K_2O-Li_2O-Al_2O_3-B_2O_3-SiO_2-MgO glasses. Series 5.

5. X-ray Analysis of Sintered Products

Sintered products were prepared by heat treatment at, or near, the temperature of the main DTA exotherm for periods inversely related to the peak height for each glass [4].

The results of the X-ray analyses of the lithia-alumino-borosilicate glasses modified by magnesia (series 2: B11 to B15) are given in table II. The principal crystalline phase in each sintered product was a β-eucryptite-type phase. With increasing MgO content, progressive small increases in the structure-cell dimensions of this phase were detected, but no numerical measurements of the actual changes were made. For

glass B15, the X-ray diffraction pattern of the β-eucryptite-type phase was more diffuse than for the other samples in the series. It is not clear whether this diffuseness originates with some inhomogeneity in composition, small particle size, or with some form of lattice strain.

Magnesium metaborate, $Mg(BO_2)_2$, constituted the major proportion of the secondary phases observed, which increased with increasing MgO content. A change in behaviour in both the temperature of the main exotherm and the softening point has been mentioned above, and it appears to coincide with the occurrence in B15 of $Mg(BO_2)_2$ as a significant phase.

The β-eucryptite-type phase present in the sintered products B 11 to B 15 has a hexagonal crystal structure with structure-cell dimensions $a_0 = 10.59$ and $c_0 = 5.48$ Å. Compared with data recorded in the literature for synthetic β-eucryptite, the *a* parameter appears to be doubled. Such doubling is required by the occurrence of several extra, superlattice reflections on the X-ray powder diffraction patterns. A specimen of β-eucryptite synthesised during the present investigations gave normal lattice parameter figures with no indication of a doubled *a* dimension, consistent with literature data. The measured structure-cell dimensions of the β-eucryptite phases observed in the various sintered products studied in the present investigation and some literature values are summarised in table IV. At present no explanation can be offered for the large *a* parameter of the phases formed in the B11 to B15 series of products.

The composition of the phase has not been precisely established for each individual sample, but it is almost certainly always quite close to $LiAlSiO_4$.

The phase constitutions of all the sintered products examined are summarised in tables II and III.

A partial replacement of the B_2O_3 content by P_2O_5 was effected, from an initial glass composition similar to B11, to give the series BP111 to BP116. Within the series, the P_2O_5 and B_2O_3 contents remained constant whilst the MgO: SiO_2 ratio was altered. The structure-cell dimensions of the β-eucryptite phase formed in these products were considerably smaller than those found in the B11 to B16 series. In addition, it was noted that progressive increases in the structure-cell dimensions and decreases in axial ratio occurred with increasing MgO content of the glass. The decrease in the structure-cell dimensions between the two series may be due to solid solution of the P_2O_5 in the β-eucryptite lattice. It is known that a quartz-like form of

TABLE IV Structure-cell dimensions for β-eucryptite-type phases formed in various sintered products.

Sample	*a*(Å)	*c*(Å)	*c*/*a*	Cell volume (Å)^3
Synthetic eucryptite; ASTM Powder Diffraction File.	5.243	5.592	1.068	133.12
Gillery and Bush (reference 6)	5.248	11.20(5.6)	2.134(1.067)	267.13(133.56)
Synthetic eucryptite prepared during present study.	5.258	5.549	1.055	132.86
B11, A23	10.59 (5.29_5)	5.48	0.517 (1.034)	532.22 (133.05)
BP111	5.179	5.474	1.057	127.15
BP116	5.22	5.48	1.049	129.31
E7, D8	5.22	5.54	1.061	130.73
B105	5.21_5	5.51	1.057	129.77

The limits of accuracy for measurements on the synthetic sample are estimated as ± 0.003 Å. In all other samples the limits are ± 0.005 Å or ± 0.01 Å, depending on the number of significant figures quoted.

$AlPO_4$ exists which has structure-cell dimensions intermediate between those of quartz and synthetic β-eucryptite. The variations in the structure-cell dimensions observed in the BP111 to BP116 series could therefore be explained by the formation of solid solutions of $AlPO_4$ in $LiAlSiO_4$. The proportion of the secondary phase detected, which is probably a type of magnesium phosphate, increases as the MgO content increases (see table III), thus decreasing the amount of $AlPO_4$ in solid solution with $LiAlSiO_4$.

Substitution of K_2O for Li_2O did not significantly alter the constitution of the crystalline materials formed on devitrification (series 5: E1 to E8; table II), which was essentially a mixture of β-eucryptite type and magnesium metaborate. The substitution did, however, affect the amount of crystalline material present in the sintered products, the amount decreasing markedly as the K_2O content of the parent glass increased. Evidence for the doubled *a* dimension of the β-eucryptite phase was obtained in only one of the products examined, otherwise the phase was similar to that observed in series 2 (B11 to B15). The structure-cell dimensions increased slightly with the increasing K_2O content. The proportion of magnesium metaborate also increased with the K_2O content of the parent glass and, in fact, constituted the major phase present in the K_2O-rich sintered products.

When the parent glasses contained large proportions of Na_2O (series 4: D1 to D8; and C133, 135), the major devitrification product was a nephelite-type phase. Within the series D1 to D8, a systematic change in the phase constitution of the sintered products from apparently single phase β-eucryptite-type to single phase nephelite-type accompanied the replacement of Li_2O by Na_2O. The term "nephelite-type" has been adopted since the phase has a similar crystal structure to the mineral nepheline, of approximate composition $K_{0.33}$ $Na_{0.67}$ $AlSiO_4$. The structure-cell dimensions of this phase were however smaller than those of the mineral, probably due to the replacement of potassium by sodium, but no actual measurements were made. No sample-to-sample variation in the cell size of the nephelite-type phase could be detected. The β-eucryptite-type phase did not have the doubled *a* dimension observed in the products B11 to B15.

A third major crystalline devitrification product, namely β-spodumene, was observed in certain sintered products. This phase has a tetragonal crystal structure and nominal composition $Li_2O.Al_2O_3.4SiO_2$. It has not been possible firmly to ascertain the compositional and treatment conditions required for the crystallisation of this phase in preference to the β-eucryptite-type, as there did not appear to be any systematic variations in the nominal compositions of the parent glasses, which did, or did not, yield β-spodumene on devitrification.

6. Correlation of DTA with X-ray Analytical Data

6.1. Series 2: B11 to B16

In fig. 3, the exotherms at 707 and 697° C for B11 and B12 appear to be characteristic of the formation of β-eucryptite-type phase. The decrease in temperature and increase in height of the exotherm through the series B13 to B16 is probably due to the co-crystallisation of magnesium metaborate, $Mg(BO_2)_2$. No endotherms were shown by B11 and B12 below 1200° C, as the compound $Li_2O.Al_2O_3.2SiO_2$ melts incongruently at 1397° C. The change in base line at ~ 1100° C for these glasses was due to the residual glassy phase becoming more fluid. The endotherms shown by B13 to B16 increased in height and temperature as the quantity of $Mg(BO_2)_2$ increased. The melting point of pure magnesium metaborate is 988° C and it is incongruent; the value of 976° C for the endotherm in B16 is in reasonable agreement with it. The other endotherms probably represent the liquidus values for eucryptite with magnesium metaborate.

6.2. Series AA 13, 23, 40, 41

The presence of the β-eucryptite-type phase can be associated with the exotherms at 720 and 710° C for AA13 and AA23, respectively, in fig. 9a. The second unidentified phase modified the peak for AA13.

However, the formation of β-spodumene gave exotherms at 835 and 840° C for AA40 and AA41, respectively, the peaks being very broad in contrast to the eucryptite peaks.

6.3. Series B101 to B105

The β-eucryptite-type phase is also shown by exotherms at ~ 720° C for these glasses in fig. 9b, but there is no indication of the presence of β-spodumene in the curve for B101. It is probable that only a very small quantity was

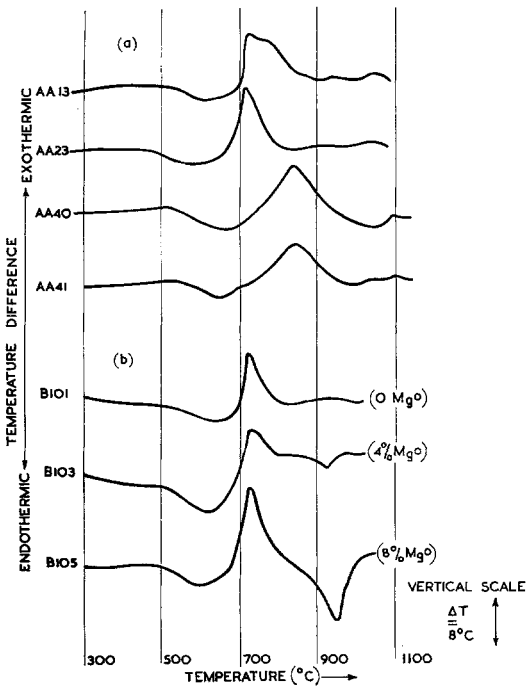

Figure 9 DTA of Li_2O-Al_2O_3-B_2O_3-SiO_2 glasses. (a) AA series; (b) B101, 103 and 105.

precipitated during the DTA run compared with that produced after 3 h treatment at 725° C for the sample prepared for X-ray analysis. The presence of magnesium metaborate is indicated by the endotherms at 920 and 950° C for B103 and B105, respectively.

6.4. Series BP111 to BP116

The exotherm for the β-eucryptite-type phase appeared at a higher temperature for the composition free from MgO (BP111), and the value then decreased from 750° C, for BP111, to 710° C, for BP114 and BP116, as the MgO content increased (fig. 10a). This behaviour was similar to that shown by B11 to B16, but differed from that shown by B101 to B105 for which no decrease was shown. The endotherms increased steadily from 930 to 1000° C, from BP112 to BP116, and corresponded to liquidi of eucryptite with an unidentified second phase, which was possibly a magnesium phosphate.

6.5. Series 4: D1 to D8

The exotherm at 753° C for D1 in fig. 6 corresponded to the formation of the nephelite-type phase which melted at 950° C. D3, D4 and D6 showed double exotherms although D5 unexpectedly did not; this may have been due by chance to poor nucleation of the second phase in this case. The peak at the lower temperature can be attributed to the β-eucryptite-type phase and this showed a progression from 738 to 654° C, the last value being influenced by a metaborate phase. The endotherms showed a continuous variation from the melting of nearly pure nephelite-type phase at 950° C, through liquidi containing progressively increasing quantities of eucryptite, to 865° C for D4. This may be close to a eutectic value for this mixture. The value of 911° C for D5 must be anomalous. As the quantity of the β-eucryptite-type phase continued to increase and the nephelite-type phase decreased to small concentrations, the endotherms again increased to 950° C for D8. This may be attributed to a liquidus of eucryptite with magnesium borate. No peak for β-spodumene was shown by D8, although a small amount of this phase was detected by X-ray analysis.

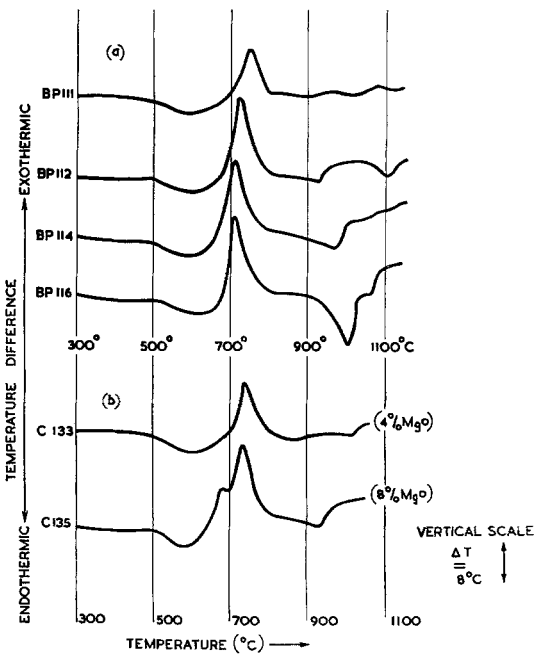

Figure 10 DTA of Li_2O-Al_2O_3-B_2O_3-SiO_2 glasses: (a) with 9.6 parts B_2O_3 replaced by an equivalent of P_2O_5. B111 series; (b) with Li_2O replaced by an equivalent of Na_2O. C133 and 135.

6.6. Series C133 to C135

The nephelite peak is shown at 735 and 730° C for C133 and C135, respectively, in fig. 10b, and a minor peak at 680° C for eucryptite in C135. The endotherms were poorly developed.

6.7. Series 5: E Glasses

The prominent features were again the exotherms for the β-eucryptite-type phase, the temperature and height of which decreased and increased, respectively, as the MgO content increased; the endotherms at ~ 940 to 960° C corresponded to the liquidi between these two compounds (fig. 8).

7. Summary

(a) Differential thermal analysis used in conjunction with softening point measurements proved to be a rapid technique in assessing solder glass composition for use in devitrifiable seals.

(b) When modified Li_2O-Al_2O_3-SiO_2 glass compositions were heat treated in the region of the respective main DTA exotherms, a β-eucryptite-type compound with composition near to $LiAlSiO_4$ crystallised as the primary phase, although the Li_2O content was relatively low and the total content of diluents, such as B_2O_3, MgO, PbO, Na_2O (see (g) below), K_2O and P_2O_5, was high. The latter were included to increase the thermal expansion.

(c) MgO, P_2O_5 and possibly B_2O_3 modify some features of the crystal structure of the β-eucryptite-type phase. For example, P_2O_5 decreased the cell size. In some cases, in the presence of MgO, the modification of the structure involved doubling the *a* lattice parameter.

(d) It appears likely that modifying ions, Mg^{2+} and P^{5+}, entered the structure of the β-eucryptite-type phase. This may have resulted from magnesium or phosphorus compounds, such as $Mg(BO_2)_2$ or P_2O_5, acting as nucleants.

(e) β-Spodumene was produced in certain sintered products, but the precise composition requirements for its formation in complex glasses have not been ascertained.

(f) The DTA exotherm for the β-eucryptite-type phase was in the range ~ 690 to 750° C and that for β-spodumene ~ 840° C. However, McMillan [1] has shown that in other modified Li_2O-Al_2O_3-SiO_2 glasses the β-spodumene exotherm occurs in the range 650 to 750° C, and the β-eucryptite exotherm at 780° C. The DTA exotherm cannot therefore be used alone to identify unambiguously the devitrifying phase.

(g) A nephelite-type primary phase devitrified from Na_2O-rich compositions when heat treated in the region of the DTA exotherm. Crystalline compounds were poorly developed from K_2O-rich compositions.

References

1. P. W. MCMILLAN, "Glass Ceramics" (Academic Press, 1964).
2. D. J. HARWOOD and L. F. OLDFIELD, British Patent Application No. 44154/63.
3. Philips Electrical Industries Ltd, British Patent 949,839 (1964).
4. Part I of this paper, *Journal of Materials Science* **1** (1966) 29.
5. ASTM Designation: C338-57.
6. F. H. GILLERY and E. A. BUSH, *J. Amer. Cer. Soc.* **42** (1959) 175.